

DYNAMIC ANALYSES OF ELASTIC PLATES WITH VOIDS

HIDEO TAKABATAKE

Kanazawa Institute of Technology, Department of Architecture, 7-1 Ogigaoka Nonoichi,
 Ishikawa 921, Japan

(Received 21 June 1989; in revised form 8 November 1990)

Abstract—A general analytical method for the dynamic response of an elastic plate with arbitrarily-disposed voids is proposed by means of the extended Dirac function. The discontinuous variation in rigidity of the plate due to the voids is expressed under the category of a continuous function by the use of the extended Dirac function. The governing equation of motion for a damped plate with voids is formulated without modifying the rigidity of the plates. The treatment is independent of the equivalent plate analogy. First, natural frequencies for a plate with voids are presented by means of the Galerkin method. The validity of the proposed natural frequencies is shown for simply-supported and clamped plates with voids through a comparison with both the results of an experiment using acrylic plates and the results obtained from the FEM code NASTRAN. Second, a dynamic analysis method based on the linear acceleration method is presented from the governing equation. The closed-form approximate solutions for a damped plate with voids are proposed for general and harmonic external loads. The validity of the closed-form approximate solutions proposed here is shown by a comparison with the numerical results obtained from the linear acceleration method and NASTRAN.

NOTATION

a	the value of the integrated natural functions
$b_{i,j}, b_{v,j}$	the widths in the x and y directions of the i, j th void, respectively
c	damping coefficient
$D(x-x_i), D(y-y_j)$	extended Dirac functions
D_0	flexural rigidity for a solid plate without voids
$d(x, y)$	rigidity ratio of plates with voids to plates without voids
E	Young's modulus
$F_{\alpha\alpha}(m, \bar{m}; i), F_{\alpha\alpha}(n, \bar{n}; j)$	integral values
f_{mn}	natural functions
$f_{m,x}, f_{n,y}$	x and y components of f_{mn}
h_0	total thickness of plate
h^*	damping constant including the effect of voids
\bar{h}	damping constant excluding the effect of voids
h	practical thickness of plate
$h_{i,j}$	height of the i, j th void
l_x, l_y	span lengths in the x and y directions
p	external lateral loads
Q_p, Q_{mn}	integral values of the external loads
w	lateral deflection on the middle surface
α	ratio of span lengths l_y to l_x
$\delta(x-x_i), \delta(y-y_j)$	Dirac functions
δ_{mn}	Kronecker delta
ν	Poisson's ratio
ρ	mass density of a plate with voids
Φ_{mn}	functions of time
$\omega_{mn}, \omega_{dmn}$	natural frequencies of undamped and damped plates with voids, respectively
ω_i	i th natural frequency of voided plates
ω_0	i th natural frequency of solid plates
ω_p	frequency of external loads.

1. INTRODUCTION

For reasons of lightness and structural efficiency and in order to guarantee enough space for equipment, plates with voids are often used in floors, roofs, bridges, etc. There are many papers discussing the analytical method for static plates with voids [for example, Holmberg (1960), Sawko and Cope (1969), Crisfield and Twemlow (1971), Cope *et al.* (1973), Elliott

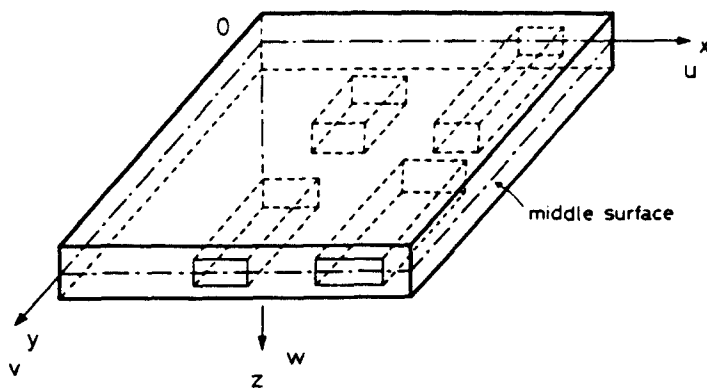


Fig. 1. Coordinates of a rectangular plate with voids.

(1978), Elliott and Clark (1982) and Cope and Clark (1984)]. However, a general analytical method for plates with arbitrarily-disposed voids has not been established. The author (Takabatake, 1991) has presented a general analytical method for such a static plate with voids by the use of an extended Dirac function. The extended Dirac function is defined as a function in which the Dirac function exists continuously in a prescribed region. For the current problem, the extended Dirac function has a value in the region where the voids exist, and replaces the discontinuous variation in the rigidity of the plates due to the voids with a continuous function; it is therefore effective in presenting a general analytical method for plates with arbitrarily-disposed voids. The theory of plates with voids is formulated without modifying the rigidity of the plates. This treatment is independent of the equivalent plate analogy. The author (Takabatake, 1987, 1988) has demonstrated the effectiveness of the extended Dirac function for analyses of tube structures with floors and of lateral buckling of I beams stiffened with stiffeners.

Dynamic problems for a plate without voids were studied by Chu and Hermann (1956) and Gorman (1982). The analysis of a dynamic plate with arbitrarily-disposed voids is based on FEM, whereas the general analytical method is scarce.

The purpose of this paper is to present a general dynamic analysis of the dynamic responses of a rectangular plate with arbitrarily-disposed voids. First, the governing equation of motion for a damped plate with voids is presented by modifying the author's result (Takabatake, 1991) for static plates with voids. The discontinuous variation in the rigidity of the plates due to the voids is expressed as a continuous function by means of the extended Dirac function. Second, the natural frequencies of a rectangular plate with voids are presented by means of the Galerkin method. The proposed solutions are examined by comparing them with experimental results using acrylic plates and with results obtained from the FEM code NASTRAN for simply-supported and clamped plates with voids. Third, the forced vibrations of a damped plate with voids are presented by the use of the linear acceleration method. For practical use, the approximate solutions for a plate with voids, subjected to general and harmonic external loads, are proposed in closed form. Last, the validity of the closed-form solutions proposed here is shown by comparing them with the numerical results obtained using the linear acceleration method and using the FEM code NASTRAN.

2. FUNDAMENTAL EQUATION OF PLATES WITH VOIDS

Consider a rectangular plate with arbitrarily-disposed voids, as shown in Fig. 1. The plate is assumed to be composed of an isotropic material. Assume that each void is a rectangular parallelepiped whose ridgelines are parallel to the x - or y -axis and which is disposed symmetrically with respect to the middle plane of the plate, as shown in Fig. 2. The position of the i, j th void is indicated by the coordinate value (x_i, y_j) of the midpoint of the void; the widths in the x and y directions of the void are $b_{x,i,j}$ and $b_{y,i,j}$, respectively;

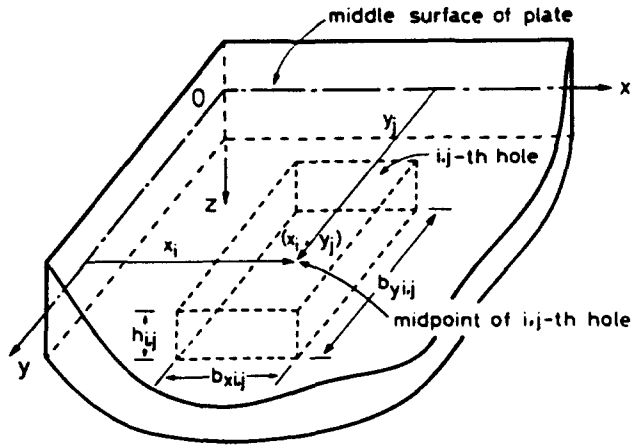


Fig. 2. Detail of a void.

and its height is $h_{i,j}$. The size and position of each void are arbitrary except for the above-mentioned assumptions.

Consider the bending problems of an isotropic plate with voids in small deformations. Since for structures like floors, roofs and bridges the height of the voids is relatively small in comparison with the thickness of the plate, the Kirchhoff-Love plate theory may be assumed to be valid for the current problem. It is also assumed that deflections of the supporting ends of the plates with voids do not occur when external loads are applied dynamically. Adding the viscous damping term to the author's theory (Takabatake, 1991) regarding the static analyses of plates with voids, the equation of motion of a rectangular plate with voids can be written as:

$$\rho h(x, y)\ddot{w} + c\dot{w} + D_0[dw_{,xx} + \nu dw_{,yy}]_{,xx} + D_0[dw_{,yy} + \nu dw_{,xx}]_{,yy} + 2(1 - \nu)D_0[dw_{,xy}]_{,xy} = p(x, y, t) \tag{1}$$

in which D_0 is the flexural rigidity for a solid plate defined as $Eh_0^3/12(1 - \nu^2)$; c is a damping coefficient; and the thickness, $h(x, y)$, and the rigidity ratio, $d(x, y)$, are given by:

$$h(x, y) = h_0 \left[1 - \sum_{i=1}^n \sum_{j=1}^m h_{i,j} D(x - x_i) D(y - y_j) \right] \tag{2}$$

$$d(x, y) = 1 - \sum_{i=1}^n \sum_{j=1}^m \alpha_{i,j} D(x - x_i) D(y - y_j). \tag{3}$$

Here h_0 is the total thickness of the plates, and the notations $D(x - x_i)$ and $D(y - y_j)$ are the extended Dirac functions defined as

$$D(x - x_i) = \begin{cases} 1 & \text{for } x_i - \frac{b_{xi,j}}{2} < x < x_i + \frac{b_{xi,j}}{2} \\ 0 & \text{for all others} \end{cases} \tag{4}$$

$$D(y - y_j) = \begin{cases} 1 & \text{for } y_j - \frac{b_{yi,j}}{2} < y < y_j + \frac{b_{yi,j}}{2} \\ 0 & \text{for all others.} \end{cases}$$

The notation $\alpha_{i,j}$ is defined as

$$\alpha_{ij} = \left(\frac{h_{i,j}}{h_0} \right)^3 \tag{5}$$

3. FREE TRANSVERSE VIBRATIONS OF A PLATE WITH VOIDS

The method of separation of variables is employed, assuming that

$$w(x, y, t) = W(x, y)\Phi(t) \tag{6}$$

in which $W(x, y)$ is a function of x and y , $\Phi(t)$ is a function of time t . Applying eqn (6) to the equation for free transverse vibrations obtained from eqn (1), the two equations satisfied by $W(x, y)$ and $\Phi(t)$ follow:

$$\ddot{\Phi}(t) + \omega^2\Phi(t) = 0 \tag{7}$$

$$[dW_{,xx}]_{,xx} + [dW_{,yy}]_{,yy} + \nu[dW_{,xy}]_{,xy} + \nu[dW_{,yx}]_{,yx} + 2(1-\nu)[dW_{,xy}]_{,xy} - \frac{\omega^2\rho h(x, y)}{D_0} = 0 \tag{8}$$

in which ω is a constant.

The natural frequencies of a plate with voids are presented by means of the Galerkin method. $W(x, y)$ is expressed by a power series expansion as follows:

$$W(x, y) = \sum_{m=1} \sum_{n=1} W_{mn} f_{mn}(x, y) \tag{9}$$

in which W_{mn} are the unknown coefficients, $f_{mn}(x, y)$ are functions satisfying the specified boundary conditions of the plates. The Galerkin equations of eqn (8) can be written as

$$\delta W_{mn} : \sum_{m=1} \sum_{n=1} W_{mn} [A_{\bar{m}\bar{n}mn} - \lambda B_{\bar{m}\bar{n}mn}] = 0 \tag{10}$$

in which the notations $A_{\bar{m}\bar{n}mn}$, $B_{\bar{m}\bar{n}mn}$ and λ are defined as

$$A_{\bar{m}\bar{n}mn} = \int_0^{l_x} \int_0^{l_y} \{ [df_{mn,xx}]_{,xx} + [df_{mn,yy}]_{,yy} + \nu[df_{mn,xy}]_{,xy} + \nu[df_{mn,xy}]_{,xy} + 2(1-\nu)[df_{mn,xy}]_{,xy} \} f_{\bar{m}\bar{n}} \, dx \, dy \tag{11}$$

$$B_{\bar{m}\bar{n}mn} = \frac{1}{l_x^4} \int_0^{l_x} \int_0^{l_y} \left[1 - \sum_{i=1} \sum_{j=1} h_{i,j} D(x-x_i) D(y-y_j) \right] f_{mn} f_{\bar{m}\bar{n}} \, dx \, dy \tag{12}$$

$$\lambda = \frac{\omega^2 \rho h_0 l_x^4}{D_0} \tag{13}$$

where the integral calculation including the extended Dirac functions, $D(x-x_i)$ and $D(y-y_j)$, is shown in the Appendix. Equations (10) are a system of linear, homogeneous, simultaneous algebraic equations with respect to the unknown displacement coefficients W_{mn} . The coefficients $B_{\bar{m}\bar{n}mn}$ appear in diagonal and non-diagonal terms due to the existence of the voids. Solving eqns (10) as eigenvalue problems for λ , the i th natural frequency, ω_i , of a plate with voids, corresponding to the i th value, λ_i , of λ , is determined from eqn (13) as

$$\omega_i = \sqrt{\lambda_i} \frac{1}{l_x^2} \sqrt{\frac{D_0}{\rho h_0}} \tag{14}$$

The natural frequencies of a plate with voids are now obtained from numerical computations. Then, approximate expressions to directly obtain the natural frequencies are considered. Although the natural frequencies are affected by the diagonal and non-diagonal terms in the square matrices $A_{\tilde{m}\tilde{n}mn}$ and $B_{\tilde{m}\tilde{n}mn}$, the main behavior is now dominated by the diagonal terms. Hence, taking only the diagonal terms in $A_{\tilde{m}\tilde{n}mn}$ and $B_{\tilde{m}\tilde{n}mn}$ into consideration, eqns (10) become of an uncoupled form. Thus the approximate values of λ are obtained as

$$\lambda_i = \frac{B_{mnmn}}{A_{mnmn}} \tag{15}$$

The approximate value for the i th natural frequency is obtained by substituting this into eqn (14).

For simply-supported plates using the following natural functions:

$$f_{mn}(x, y) = \sin \frac{m\pi x}{l_x} \sin \frac{n\pi y}{l_y} \tag{16}$$

the coefficients $A_{\tilde{m}\tilde{n}mn}$ and $B_{\tilde{m}\tilde{n}mn}$ are

$$\begin{aligned} A_{mnmn} = & \pi^4 \left[m^2 + \left(\frac{n}{\alpha} \right)^2 \right]^2 \delta_{m\tilde{m}} \delta_{n\tilde{n}} \\ & - \sum_{i=1} \sum_{j=1} 4\pi^4 \alpha_{ij} \left[F_{xss}(m, \tilde{m}; i) F_{yss}(n, \tilde{n}; j) \left[m^2 + \left(\frac{n}{\alpha} \right)^2 \right] \right. \\ & - 2m \left[m^2 + \left(\frac{n}{\alpha} \right)^2 \right] [mF_{xss}(m, \tilde{m}; i) - \tilde{m}F_{xcc}(m, \tilde{m}; i)] F_{yss}(n, \tilde{n}; j) \\ & - 2 \left[\left(\frac{n}{\alpha} \right)^3 + m^2 \frac{n}{\alpha} \right] \left[\frac{n}{\alpha} F_{yss}(n, \tilde{n}; j) - \frac{n}{\alpha} F_{ycc}(n, \tilde{n}; j) \right] F_{xss}(m, \tilde{m}; i) \\ & + \left[m^2 + \nu \left(\frac{n}{\alpha} \right)^2 \right] \{ [m^2 + \tilde{m}^2] F_{xss}(m, \tilde{m}; i) - 2m\tilde{m}F_{xcc}(m, \tilde{m}; i) \} F_{yss}(n, \tilde{n}; j) \\ & + \left[\left(\frac{n}{\alpha} \right)^2 + \nu m^2 \right] \left\{ \left[\left(\frac{n}{\alpha} \right)^2 + \left(\frac{\tilde{n}}{\alpha} \right)^2 \right] F_{yss}(n, \tilde{n}; j) - 2 \frac{n}{\alpha} \frac{\tilde{n}}{\alpha} F_{ycc}(n, \tilde{n}; j) \right\} F_{xss}(m, \tilde{m}; i) \\ & + 2(1 - \nu)m \frac{n}{\alpha} [mF_{xss}(m, \tilde{m}; i) - \tilde{m}F_{xcc}(m, \tilde{m}; i)] \left[\frac{n}{\alpha} F_{yss}(n, \tilde{n}; j) + \frac{\tilde{n}}{\alpha} F_{ycc}(n, \tilde{n}; j) \right] \end{aligned} \tag{17}$$

$$B_{\tilde{m}\tilde{n}mn} = \delta_{\tilde{m}m} \delta_{\tilde{n}n} - 4 \sum_{i=1} \sum_{j=1} \left(\frac{h_{i,j}}{h_0} \right) F_{xss}(m, \tilde{m}; i) F_{yss}(n, \tilde{n}; j) \tag{18}$$

in which $\alpha = l_y/l_x$; $\delta_{m\tilde{m}}$ and $\delta_{n\tilde{n}}$ are the Kronecker deltas; and the notations $F_{xss}(m, \tilde{m}; i)$ and $F_{xcc}(m, \tilde{m}; i)$ are defined as

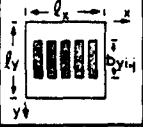
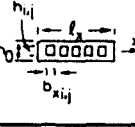
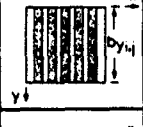
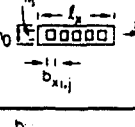
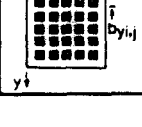
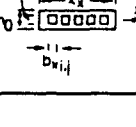
$$\begin{aligned} \begin{Bmatrix} F_{\text{css}}(m, \bar{m}; i) \\ F_{\text{ccc}}(m, \bar{m}; i) \end{Bmatrix} &= \frac{1}{l_x} \int_{x_i - (b_{xij}/2)}^{x_i + (b_{xij}/2)} \begin{Bmatrix} \sin\left(\frac{m\pi x}{l_x}\right) \sin\left(\frac{\bar{m}\pi x}{l_x}\right) \\ \cos\left(\frac{m\pi x}{l_x}\right) \cos\left(\frac{\bar{m}\pi x}{l_x}\right) \end{Bmatrix} dx \\ &= \frac{1}{(m - \bar{m})\pi} \cos\left(\frac{(m - \bar{m})\pi x_i}{l_x}\right) \sin\left(\frac{(m - \bar{m})\pi b_{xij}}{2l_x}\right) (1 - \delta_{m\bar{m}}) + \frac{1}{2} \left(\frac{b_{xij}}{l_x}\right) \delta_{m\bar{m}} \\ &\quad \mp \frac{1}{(m + \bar{m})\pi} \cos\left(\frac{(m + \bar{m})\pi x_i}{l_x}\right) \sin\left(\frac{(m + \bar{m})\pi b_{xij}}{2l_x}\right). \end{aligned} \quad (19)$$

The notations $F_{\text{yss}}(n, \bar{n}; j)$ and $F_{\text{ycc}}(n, \bar{n}; j)$ were obtained by making the substitutions $m \rightarrow n$, $\bar{m} \rightarrow \bar{n}$, $x_i \rightarrow y_j$, $b_{xij} \rightarrow b_{yij}$ and $l_x \rightarrow l_y$ in eqn (19). On the other hand, the natural frequencies for clamped rectangular plates with voids were obtained similarly by using suitable natural functions for clamped solid plates.

4. NUMERICAL RESULTS FOR NATURAL FREQUENCIES

The natural frequencies for a plate with voids have been presented by means of the Galerkin method. In order to examine the natural frequencies proposed here, numerical computations were carried out for three cases, as shown in Table 1. All the voids have the same cross-section spaced equally. Figures 3-5 and 6-8 show the first natural frequencies for simply-supported and clamped plates with voids, respectively, in which Poisson's ratio, ν , is 0.17; the width-span ratios, b_{xij}/l_x and b_{yij}/l_y , of the i, j th void take the values 0.05, 0.10 and 0.15; the ratios h_{ij}/h_0 change from 0 to 0.9; and the aspect ratio, l_y/l_x , is always 1.0. The value at $h_{ij}/h_0 = 0$ indicates the value for normal solid plates without voids. In these figures each first natural frequency, ω_1 , is divided by the first natural frequency, ω_{01} , of the solid plates. The numerical results show that the differences between the results obtained using eqn (10) and the approximate results obtained using eqn (15) are too small to plot and are negligible in practical use. The results obtained from the proposed theory show excellent agreement when compared with results obtained from the FEM code NASTRAN, in which 22×22 finite elements are used. However, the ratio h_{ij}/h_0 in these figures must be restricted to being smaller than 0.6 due to the use of the Kirchhoff-Love assumption made here. In this calculation, the natural functions for fixed plates with voids use, for the sake of computational simplicity, the following approximate expressions:

Table 1. Lists of isotropic rectangular plates with voids

TYPE	PLANE	SECTION	$\frac{h_{ij}}{h_0}$	$\frac{b_{xij}}{l_x}$	$\frac{b_{yij}}{l_y}$	$\alpha = \frac{l_y}{l_x}$
1			0.5	0.1	0.5	1.0
2			0.5	0.1	1.0	1.0
3			0.5	0.1	0.1	1.0

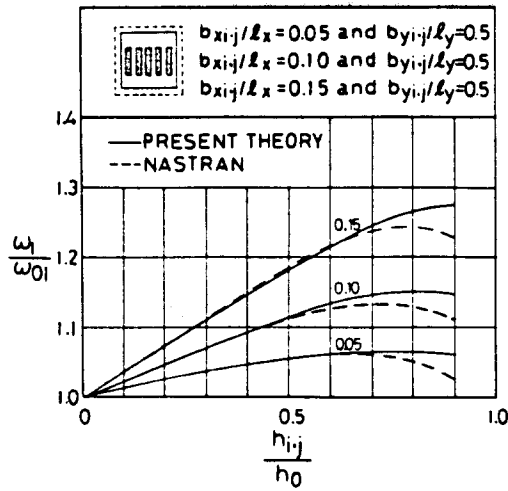


Fig. 3. The first natural frequency of a simply-supported plate with voids (Type 1).

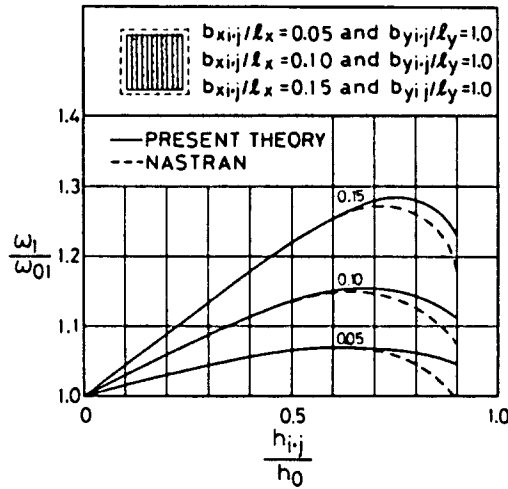


Fig. 4. The first natural frequency of a simply-supported plate with voids (Type 2).

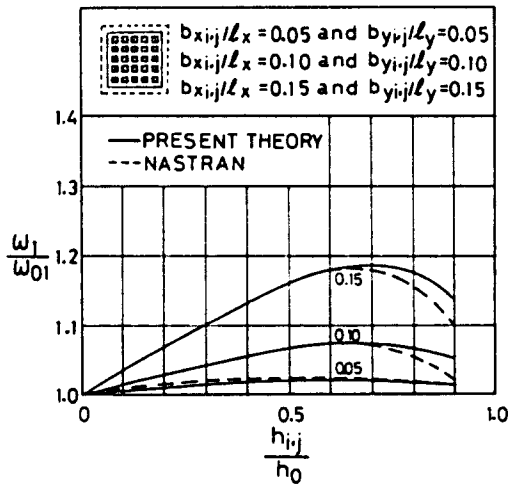


Fig. 5. The first natural frequency of a simply-supported plate with voids (Type 3).

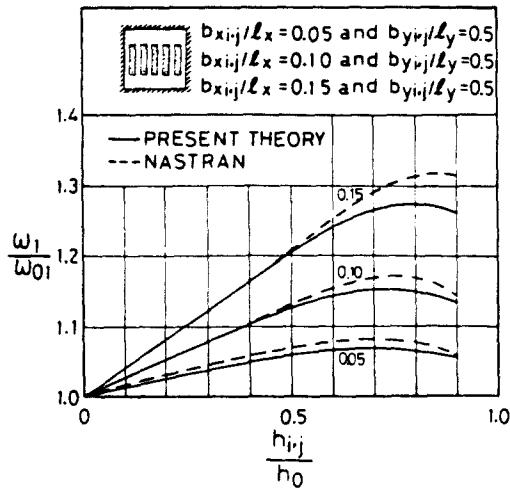


Fig. 6. The first natural frequency of a clamped plate with voids (Type 1).

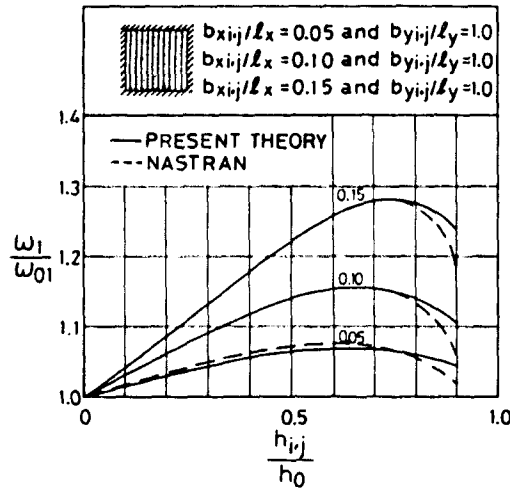


Fig. 7. The first natural frequency of a clamped plate with voids (Type 2).

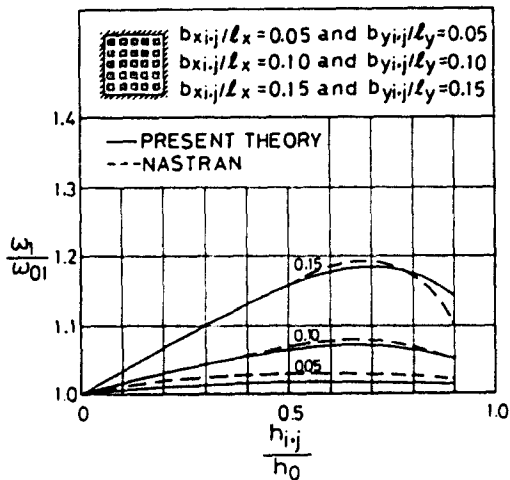


Fig. 8. The first natural frequency of a clamped plate with voids (Type 3).

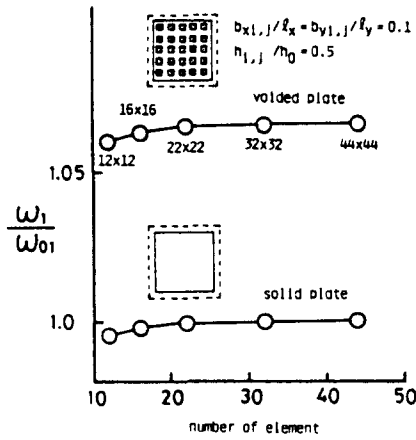


Fig. 9. Convergence of finite elements with mesh refinement.

$$f_{mn}(x, y) = \sin\left(\frac{\pi x}{l_x}\right) \sin\left(\frac{m\pi x}{l_x}\right) \sin\left(\frac{\pi y}{l_y}\right) \sin\left(\frac{n\pi y}{l_y}\right). \tag{20}$$

If the well-known exact natural functions for normal plates are used, the results of the numerical computation for fixed plates with voids will be improved.

Figure 9 shows the convergence of the finite elements with mesh refinement on the natural frequencies of the simply-supported plate with voids, named Type 3, and the solid plate. It follows that the 22 × 22 elements used in the above comparison are appropriate for good convergence.

For higher natural frequencies the proposed theory also shows good agreement with the results obtained from NASTRAN. The higher natural frequencies increase in proportion to the increase in the ratio $h_{1,j}/h_0$. The behavior is the same as the first natural frequency for $h_{1,j}/h_0$ smaller than 0.6, except for the second, fourth, etc. natural frequencies of simply-supported plates and fixed plates named Type 1. These differences are caused when the natural modes of Type 1 are asymmetric with respect to a line given by $y = l_y/2$ which passes through the midspan, as shown in Fig. 10. For these modes of Type 1 the position of the voids is such that they occur on a part of, but not throughout, the span of the plate with respect to the line $y = l_y/2$. Therefore, the effects of the voids on these natural modes cancel each other, and the increment of these natural frequencies due to the voids is less than for the other modes of Type 1 and other types. Figure 11 shows the second natural frequency for simply-supported plates with voids.

5. RELATIONSHIPS BETWEEN THEORETICAL RESULTS AND EXPERIMENTAL RESULTS FOR NATURAL FREQUENCIES

In order to examine experimentally the theory proposed here, experiments for acrylic plates with voids were carried out for both simply-supported and clamped cases.

The experimental equipment is shown schematically in Fig. 12. The span lengths $l_x = l_y = 30$ cm (11.81 in). The material constants are Young's modulus $E = 32,700$ kgf cm⁻² (465,100 lb in⁻²), Poisson's ratio $\nu = 0.34$, and mass density $\rho = 1.199 \times 10^{-6}$ kgf s² cm⁻⁴ (1.096×10^{-10} lb s² in⁻⁴). The natural frequencies are calculated from the dynamical deflections at the midpoint of the specimens. The relationships for the first natural frequency between the experimental results and the theoretical results proposed here are shown in Table 2. It shows that the proposed theory agrees well with the experimental results. Thus, although the specimens are insufficient in number, it is shown that the proposed theory can apply in practice to plates with voids.

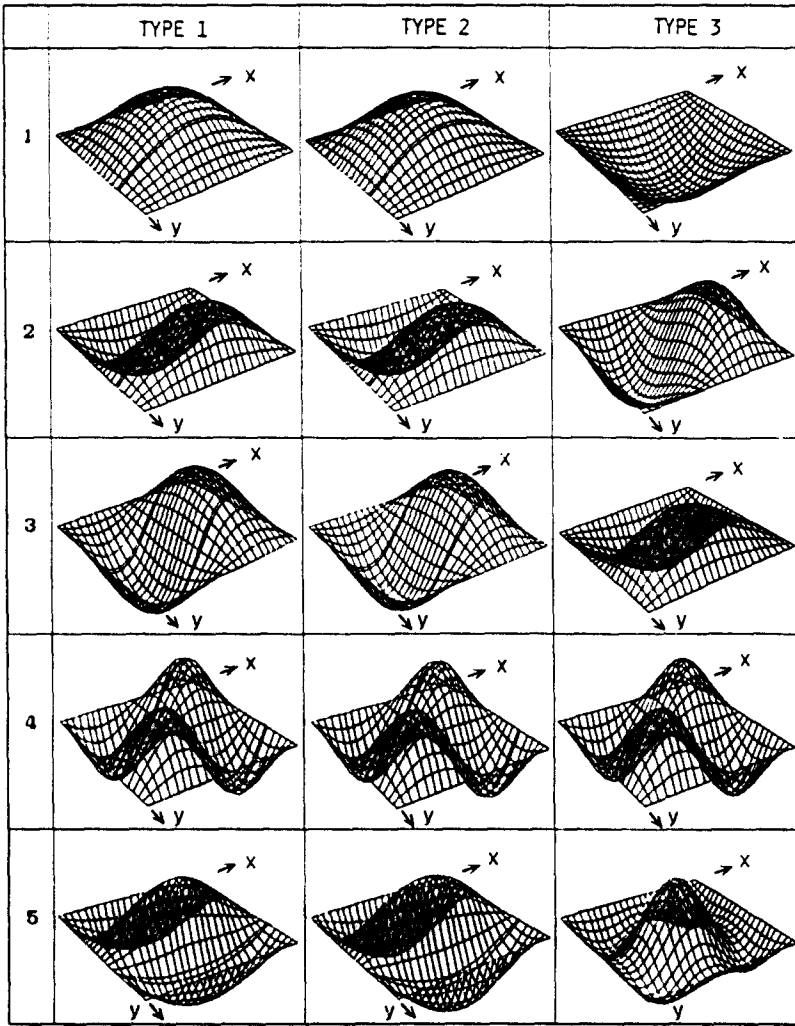


Fig. 10. Frequency modes of simply-supported plates with voids.

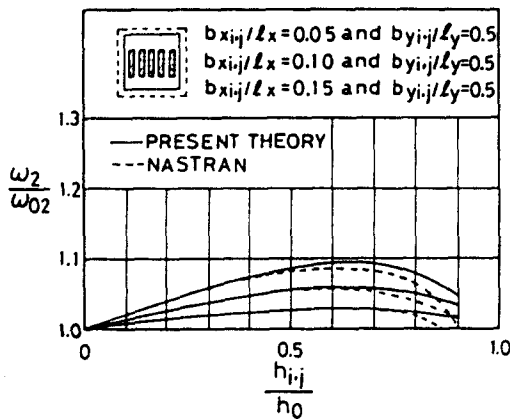


Fig. 11. The second natural frequency of a simply-supported plate with voids (Type 1).

6. FORCED VIBRATIONS OF PLATES WITH VOIDS

Free transverse vibrations of a plate with voids have been presented. Next, forced vibrations of plates with voids will be considered. The general solution of eqn (1) is assumed to be of the form

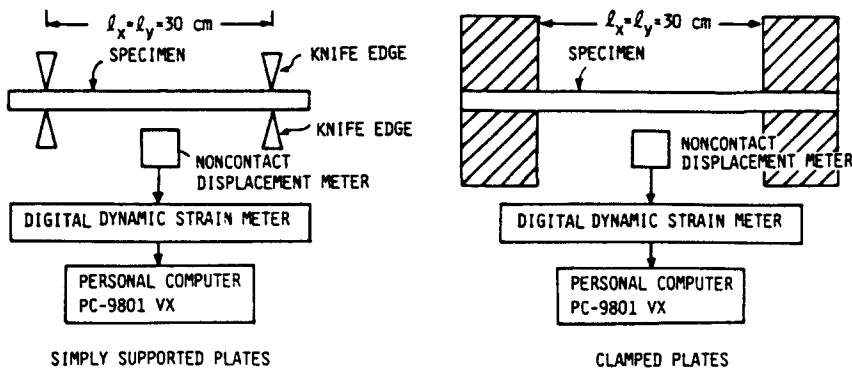


Fig. 12. Schematic diagram of the experimental equipment.

Table 2. Relationships between the theoretical and experimental results

Type	$h_{c,d}/h_0$	$b_{c,d}/l_x$	$h_{c,d}/l_y$		First natural frequencies	
					Simply-supported plate	Clamped plate
0	0	0	0	Experiment	720.8 rad s ⁻¹	1296.3 rad s ⁻¹
				Theory	666.5 rad s ⁻¹	1257.8 rad s ⁻¹
				Error	7.5%	2.9%
1	0.33	0.1	0.5	Experiment	746.3 rad s ⁻¹	1344.8 rad s ⁻¹
				Theory	738.2 rad s ⁻¹	1439.4 rad s ⁻¹
				Error	1.0%	-7.0%
2	0.33	0.1	1.0	Experiment	755.7 rad s ⁻¹	1320.9 rad s ⁻¹
				Theory	758.5 rad s ⁻¹	1464.7 rad s ⁻¹
				Error	-0.4%	-10.8%
3	0.33	0.1	0.1	Experiment	729.0 rad s ⁻¹	1399.0 rad s ⁻¹
				Theory	723.9 rad s ⁻¹	1423.2 rad s ⁻¹
				Error	0.7%	-1.7%

Error = (Experiment - Theory)/(Experiment); $\alpha = l_x/l_y = 1.0$; $l_x = 30$ cm; and $h_0 = 0.6$ cm

$$w(x, y, t) = \sum_{m=1}^{\infty} \sum_{n=1}^{\infty} f_{mn}(x, y) \Phi_{mn}(t) \tag{21}$$

in which $\Phi_m(t)$ are unknown functions of time t ; and the functions $f_{mn}(x, y)$ are the natural functions satisfying both the differential eqns (8) and the specified boundary conditions at the ends of the plate. Substituting eqn (21) into eqn (1) and using the eqn (8), we have

$$\sum_{m=1}^{\infty} \sum_{n=1}^{\infty} f_{mn}(x, y) [\rho h(x, y) \ddot{\Phi}_{mn}(t) + c \dot{\Phi}_{mn}(t) + \rho h(x, y) \omega_{mn}^2 \Phi_{mn}(t)] = p(x, y, t). \tag{22}$$

Since the thickness $h(x, y)$ is a function of x and y , eqn (22) cannot be transformed into an uncoupled form by means of the orthogonality relations for natural functions. Therefore, eqn (22) will be solved by either numerical computation based on the Wilson- θ method in Section 7 or the approximate closed-form solution in Section 8.

7. DYNAMIC ANALYSES BASED ON THE LINEAR ACCELERATION METHOD

Since eqn (22) is in a coupled form, the solution is presented from the numerical computations. Multiplying both sides of eqn (22) by $f_{mn}(x, y)$ and integrating between 0 to l_x and 0 to l_y , eqn (22) reduces to

$$\sum_{m=1}^{\infty} \sum_{n=1}^{\infty} \left\{ K_{\dot{m}\dot{n}m\dot{n}} [\ddot{\Phi}_{mn} + \omega_{mn}^2 \Phi_{mn}] + \frac{c}{\rho h_0} \delta_{m\dot{m}\dot{n}} \delta_{n\dot{n}} \dot{\Phi}_{mn} \right\} = \frac{Q_{mn}(t)}{\alpha \rho h_0} \tag{23}$$

in which the notations $K_{\dot{m}\dot{n}m\dot{n}}$, $Q_{mn}(t)$ and a are defined as

$$K_{\bar{m}\bar{m}mn} = \delta_{\bar{m}\bar{m}}\delta_{\bar{n}\bar{n}} - \frac{l_x l_y}{a} \sum_{i=1}^{l_x} \sum_{j=1}^{l_y} \left(\frac{h_{i,j}}{h_0} \right) F_x(m, \bar{m}; i) F_y(n, \bar{n}; j) \tag{24}$$

$$Q_{mn}(t) = \int_0^{l_x} \int_0^{l_y} p(x, y, t) f_{\bar{m}\bar{n}}(x, y) dx dy \tag{25}$$

$$a = \int_0^{l_x} \int_0^{l_y} f_{mn}(x, y) f_{mn}(x, y) dx dy \tag{26}$$

in which the non-dimensional quantities $F_x(m, \bar{m}; i)$ and $F_y(n, \bar{n}; j)$ are defined as

$$F_x(m, \bar{m}; i) = \frac{1}{l_x} \int_0^{l_x} D(x-x_i) f_{vm} f_{v\bar{m}} dx \tag{27}$$

$$F_y(n, \bar{n}; j) = \frac{1}{l_y} \int_0^{l_y} D(y-y_j) f_{vn} f_{v\bar{n}} dy. \tag{28}$$

The notations f_{vm} and f_{vn} are the x and y components of f_{mn} , respectively. Equation (23) can be solved by using the Wilson- θ method. The current natural functions $f_{mn}(x, y)$ take eqn (16) for a simply-supported plate with voids and eqn (20) for a clamped plate with voids.

8. CLOSED-FORM APPROXIMATE SOLUTIONS FOR FORCED VIBRATIONS

The dynamic analysis for a damped plate with voids has been presented by means of the linear acceleration method. Then, for practical use, consider an approximation of the closed-form solution for a damped plate with voids.

The dynamical response of a plate with voids is obtained by solving eqn (23). Since the coefficients $K_{\bar{m}\bar{m}mn}$ in eqn (23) have non-diagonal terms $m \neq \bar{m}$ and/or $n \neq \bar{n}$ due to the effect of the voids, eqn (23) takes on a coupled form. Assuming that the behavior of a plate with voids is now dominated by the diagonal terms in the coefficients $K_{\bar{m}\bar{m}mn}$, eqn (23) becomes of an uncoupled form. The effectiveness of the assumption used here has been numerically demonstrated in the presentation of the approximate solutions for natural frequencies of a plate with voids. Thus, eqn (23) can be approximated as

$$\ddot{\Phi}_{mn}(t) + \frac{c}{\rho h_0 K_{\bar{m}\bar{m}mn}} \dot{\Phi}_{mn}(t) + \omega_{mn}^2 \Phi_{mn}(t) = \frac{Q_{mn}(t)}{a \rho h_0 K_{\bar{m}\bar{m}mn}}. \tag{29}$$

Now, the damping constants, h^* , are defined as

$$\frac{c}{\rho h_0 K_{\bar{m}\bar{m}mn}} = 2h^* \omega_{mn}. \tag{30}$$

They include the effect of the voids since the term $K_{\bar{m}\bar{m}mn}$ includes the effect of the voids. The relations between the damping constants, h^* , and usual damping constants, \tilde{h} , excluding the effect of the voids, are given by

$$\tilde{h} = h^* K_{\bar{m}\bar{m}mn} \tag{31}$$

in which h is defined as

$$\frac{c}{\rho h_0} = 2\tilde{h}\omega_{mn}. \tag{32}$$

The damping constants, h^* , depend on the values of m and n . Hence the substitution of eqn (30) into eqn (29) results in

$$\ddot{\Phi}_{mn}(t) + 2h^*\omega_{mn}\dot{\Phi}_{mn}(t) + \omega_{mn}^2\Phi_{mn}(t) = \frac{Q_{mn}}{a\rho h_0 K_{mnmn}}. \tag{33}$$

The general solution of eqn (33) is

$$\begin{aligned} \Phi_{mn}(t) = & \exp(-h^*\omega_{mn}t)[C_1 \sin \omega_{Dmn}t + C_2 \cos \omega_{Dmn}t] \\ & + \frac{1}{a\rho h_0 K_{mnmn}\omega_{Dmn}} \int_0^t \exp[-h^*\omega_{mn}(t-\tau)] \sin \omega_{Dmn}(t-\tau) Q_{mn}(\tau) d\tau \end{aligned} \tag{34}$$

in which ω_{mn} are the natural frequencies of the undamped plates with voids; and ω_{Dmn} are the natural frequencies of the damped plates with voids. The relationship between ω_{mn} and ω_{Dmn} is

$$\omega_{Dmn} = \omega_{mn}\sqrt{1-h^{*2}}. \tag{35}$$

Hence the dynamic deflections of plates with voids are determined by substituting eqn (34) into eqn (21).

Next, consider the dynamic solutions of a plate with voids, subjected to the following harmonic external load:

$$p(x, y, t) = p_{iv}(x, y) \sin \omega_p t \tag{36}$$

in which $p_{iv}(x, y)$ is a function of the external loads, and ω_p is the frequency of the external loads. Then the notation $Q_{mn}(t)$ can be written as

$$Q_{mn}(t) = \sin \omega_p t Q_p(m, n) \tag{37}$$

in which the $Q_p(m, n)$ are defined as

$$Q_p(m, n) = \int_0^{l_x} \int_0^{l_y} p_{iv}(x, y) f_{mn}(x, y) dx dy. \tag{38}$$

If at $t = 0$

$$w(x, y, 0) = 0, \quad \dot{w}(x, y, 0) = 0 \tag{39}$$

then $\Phi_{mn}(t)$ become

$$\begin{aligned} \Phi_{mn}(t) = & \frac{Q_p(m, n)}{a\rho h_0 K_{mnmn}\omega_{Dmn}} \frac{1}{2} \left\{ \frac{h^*\omega_{mn} \cos(\omega_p t) + (\omega_p + \omega_{Dmn}) \sin(\omega_p t)}{(h^*\omega_{mn})^2 + (\omega_p + \omega_{Dmn})^2} \right. \\ & - \frac{h^*\omega_{mn} \cos(\omega_p t) + (\omega_p - \omega_{Dmn}) \sin(\omega_p t)}{(h^*\omega_{mn})^2 + (\omega_p - \omega_{Dmn})^2} \\ & + \exp(-h^*\omega_{mn}t) \left[\frac{(\omega_p + \omega_{Dmn}) \sin(\omega_{Dmn}t) - h^*\omega_{mn} \cos(\omega_{Dmn}t)}{(h^*\omega_{mn})^2 + (\omega_p + \omega_{Dmn})^2} \right. \\ & \left. \left. + \frac{(\omega_p - \omega_{Dmn}) \sin(\omega_{Dmn}t) + h^*\omega_{mn} \cos(\omega_{Dmn}t)}{(h^*\omega_{mn})^2 + (\omega_p - \omega_{Dmn})^2} \right] \right\}. \end{aligned} \tag{40}$$

Thus the closed-form approximate solutions for a damped plate with voids have been presented. The closed-form solution for undamped plates with voids is given by setting, as $h^* \rightarrow 0$, $\omega_{Dmn} \rightarrow \omega_{mn}$ and $\exp(-h^*\omega_{mn}t) \rightarrow 1$ in eqns (34) and (40), while the solution for solid plates without voids is obtained by replacing K_{mmmn} with 1.

9. NUMERICAL RESULTS FOR DYNAMICAL RESPONSES: DISCUSSIONS

To examine the approximate solution proposed here for an isotropic rectangular plate with voids, numerical computations were carried out for three cases, as shown in Table 1. The data used are as follows: Young's modulus $E = 2.1 \times 10^6 \text{ tf m}^{-2}$ ($2.987 \times 10^6 \text{ lb in}^{-2}$); Poisson's ratio $\nu = 0.17$; thickness $h_0 = 0.3 \text{ m}$ (0.984 ft); span lengths $l_x = l_y = 10 \text{ m}$ (32.808 ft); voided ratio $h_{i,j}/h_0 = 0.5$; and mass density $\rho = 244.9 \text{ kgf s}^{-2} \text{ m}^{-4}$ ($4.660 \text{ lb s}^{-2} \text{ ft}^{-4}$). The external lateral load is assumed to be a harmonic and uniformly-distributed force given in eqn (36), in which $p_{xy}(x, y) = 0.15 \text{ tf m}^{-2}$ (30.7 lb ft^{-2}) and $\omega_p = \omega_{01} \cdot 2$. Here ω_{01} is the first natural frequency for solid plates without voids.

Figures 13–15 show the dynamic deflections at the midpoint of simply-supported plates with voids of Types 1–3, respectively, while Figs 16–18 show the dynamic deflections at the

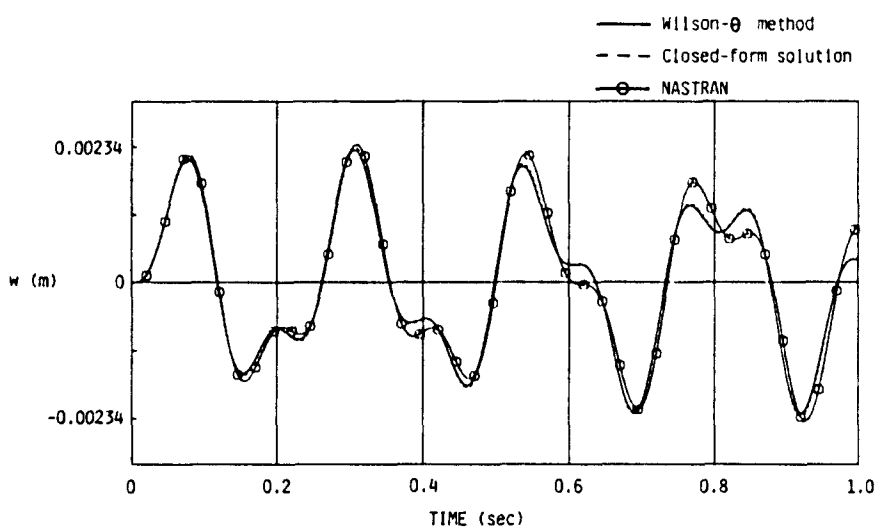


Fig. 13. Dynamic deflections w for a simply-supported plate with voids (Type 1).

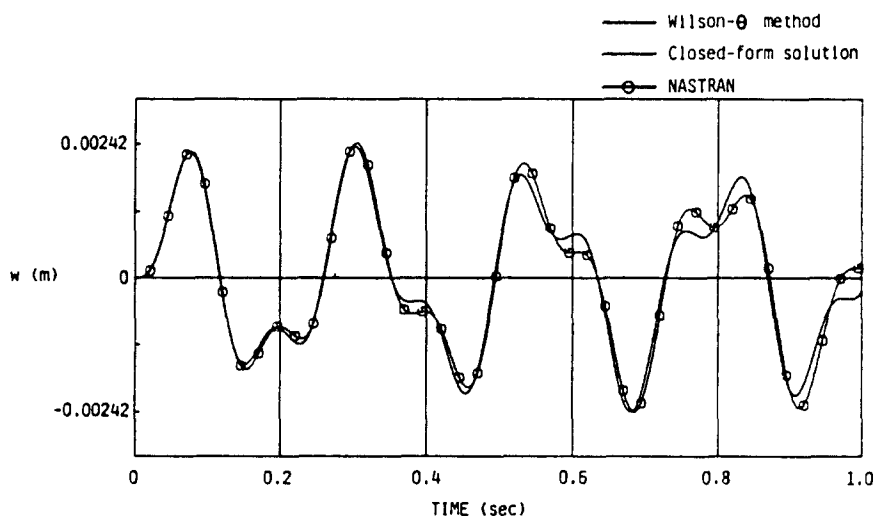


Fig. 14. Dynamic deflections w for a simply-supported plate with voids (Type 2).

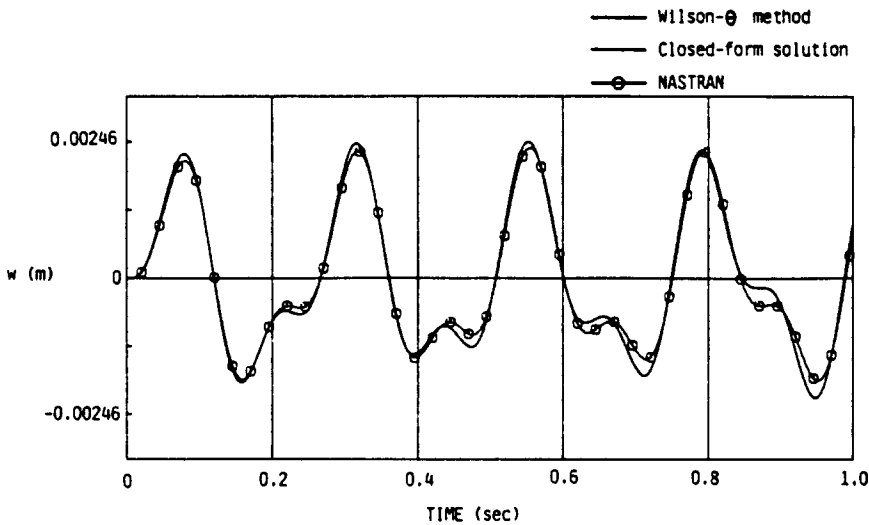


Fig. 15. Dynamic deflections w for a simply-supported plate with voids (Type 3).

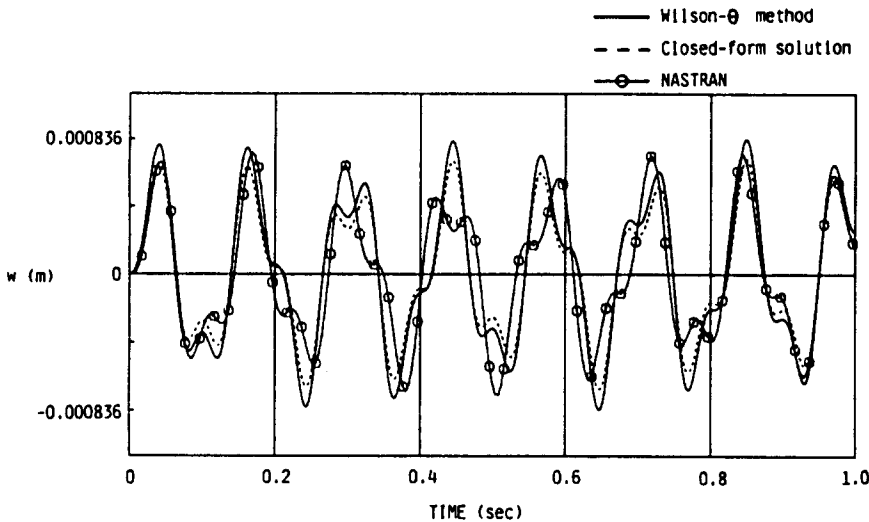


Fig. 16. Dynamic deflections w for a clamped plate with voids (Type 1).

midpoint of clamped plates with voids of Types 1–3, respectively. In these figures, the solid lines indicate values obtained from the numerical computations using the linear acceleration method; the broken lines indicate values obtained from the closed-form approximate solution; and the solid lines with circles indicate values obtained from the FEM code NASTRAN. The numerical results show that the closed-form approximate solution proposed here is applicable to the dynamic analyses of plates with voids, in practical use.

The limitation of the ratio h_{v1}/h_0 in the proposed theory on natural frequencies has already been stated as being smaller than 0.6. This limitation is also effective for dynamic plates with voids, subjected to forced vibrations, because the inaccuracy of the natural frequencies results in an inexact dynamical response.

On the other hand, the limitation of the ratios b_{x1}/l_x and b_{y1}/l_y is not clear. They are restricted by the shear forces and the validity of the Kirchhoff–Love plate theory. West (1973) suggests that cell distortion of a plate with voids should be taken into account when the void area exceeds 60% of the total cross-section.

For the sake of simplicity, this paper disregards the transverse shear deformation and the local deformation of the top and bottom platelets of the void. It will be necessary to consider these deformations when the cross-section and/or number of voids increases. The

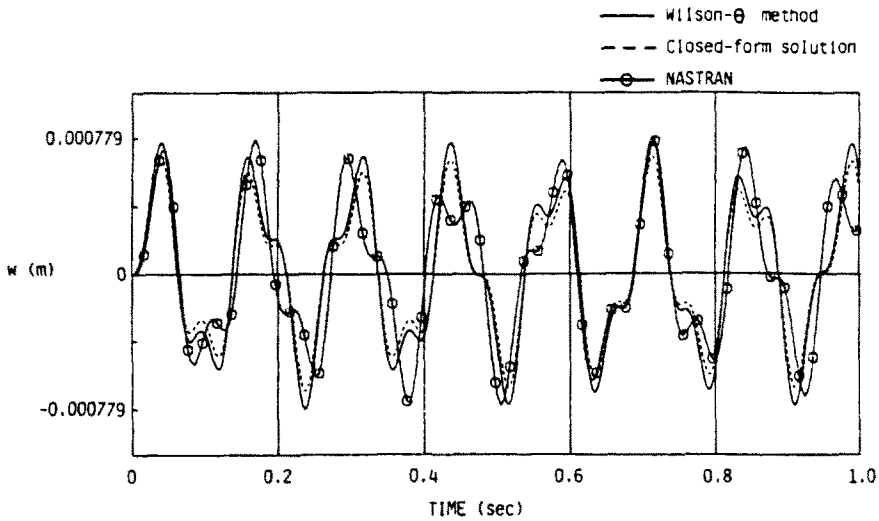


Fig. 17. Dynamic deflections w for a clamped plate with voids (Type 2).

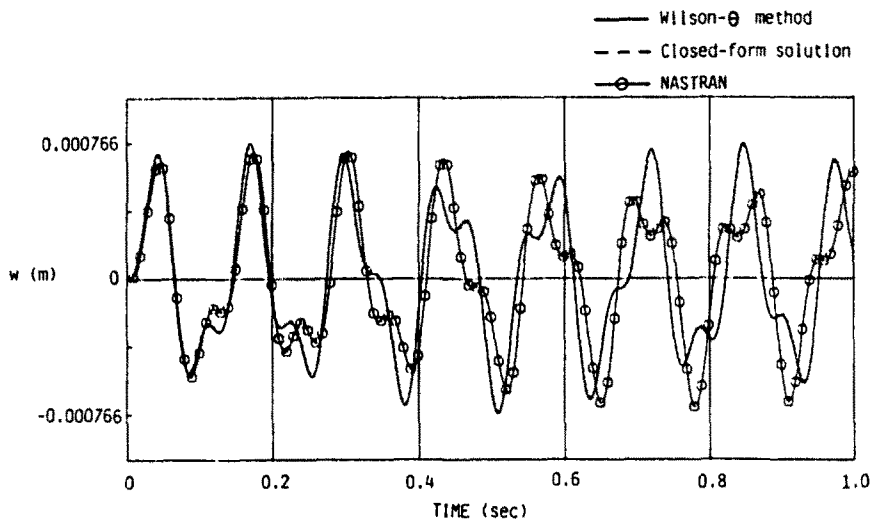


Fig. 18. Dynamic deflections w for a clamped plate with voids (Type 3).

transverse shear deformation can be considered by replacing the Kirchhoff-Love plate hypotheses with the Mindlin plate theory.

Each void was assumed to be a rectangular parallelepiped for simplicity's sake, but it is relatively easy to extend the proposed theory to a void with circular or symmetric cross-section.

10. CONCLUSIONS

The general analysis methods and closed-form approximate solutions for free and forced vibrations of an isotropic rectangular plate with arbitrarily-disposed voids have been proposed by means of the extended Dirac function. The closed-form solutions proposed here have been validated by comparing them with the numerical results obtained from the linear acceleration method proposed here and from the FEM code NASTRAN and with the experimental results.

Acknowledgements—The author wishes to thank the Takamatsu Construction Company for the financial support for this investigation. He would like to express his appreciation to O. Yamada and T. Matsuura of Kanazawa Institute of Technology for their help in verifying the computer programs.

REFERENCES

Chu, H. N. and Hermann, G. (1956). Influence of large amplitudes on free flexural vibrations of rectangular elastic plates. *J. Appl. Mech. ASME* **23**, 532-540.

Cope, R. J. and Clark, L. A. (1984). *Concrete Slabs—Analysis and Design*. Elsevier Applied Science, London.

Cope, R. J., Harris, G. and Sawko, F. (1973). A new approach to the analysis of cellular bridge decks. *Analysis of Structural Systems for Torsion*, ACI., Sp 35-5, pp. 185-210.

Crisfield, M. A. and Twemlow, R. P. (1971). The equivalent plate approach for the analysis of cellular structures. *Civil Engineering and Public Works Review*, March, pp. 259-263.

Elliott, G. (1978). Partial loading on orthotropic plates. Cement and Concrete Association Technical Report 42, p. 519, London.

Elliott, G. and Clark, L. A. (1982). Circular voided concrete slab stiffness. *J. Struct. Div. ASCE* **108**(11), 2379-2393.

Gorman, D. J. (1982). *Free Vibration Analysis of Rectangular Plates*. Elsevier-North Holland, Amsterdam.

Holmberg, A. (1960). *Shear-weak Beams on Elastic Foundation*, Vol. 10. International Association for Bridge and Structural Engineering (IABSE), Zurich.

Sawko, F. and Cope, R. J. (1969). Analysis of multi-cell bridges without transverse diaphragms—a finite element approach. *Structural Engng* **47**(112), 455-460.

Takabatake, H. (1987). Bending and torsional analyses of tube systems (in Japanese). *Proc. Symp. on Computational Methods in Structural Engineering and Related Fields*, Vol. 11, pp. 205-210.

Takabatake, H. (1988). Lateral buckling of I beams with web stiffeners and batten plates. *Int. J. Solids Structures* **24**(10), 1003-1019.

Takabatake, H. (1991). Static analyses of elastic plates with voids. *Int. J. Solids Structures* **28**(2), 179-196.

West, R. (1973). Recommendations on the use of grillage analysis for slabs and pseudo-slab bridge decks. Report 46.017, Cement and Concrete Association, and Construction Industry Research and Information Association, London.

APPENDIX. INTEGRAL CALCULATION INCLUDING THE EXTENDED DIRAC FUNCTION

The integral calculation including the extended Dirac function $D(x-x_i)$ for a given function $f(x)$ can be written as:

$$\int_0^l D(x-x_i)f(x) dx = \int_{x_i-(h_{i,j}/2)}^{x_i+(h_{i,j}/2)} [\delta(x-\xi)f(x) dx] d\xi = \int_{x_i-(h_{i,j}/2)}^{x_i+(h_{i,j}/2)} f(\xi) d\xi \tag{A1}$$

in which ξ is a supplementary variable of x . Similarly,

$$\int_0^l D(y-y_j)f(y) dy = \int_{y_j-(h_{i,j}/2)}^{y_j+(h_{i,j}/2)} f(\eta) d\eta \tag{A2}$$

in which η is a supplementary variable of y . The n th derivatives of the extended Dirac functions can therefore be expressed as

$$\int_0^l D^{(n)}(x-x_i)f(x) dx = \int_{x_i-(h_{i,j}/2)}^{x_i+(h_{i,j}/2)} (-1)^n f^{(n)}(\xi) d\xi$$

$$\int_0^l D^{(n)}(y-y_j)f(y) dy = \int_{y_j-(h_{i,j}/2)}^{y_j+(h_{i,j}/2)} (-1)^n f^{(n)}(\eta) d\eta \tag{A3}$$

in which superscripts enclosed within parentheses indicate the differential order.

When the conditions $h_{i,j} \ll l_i$ and $h_{i,j} \ll l_j$ are satisfied, the extended Dirac functions $D(x-x_i)$ and $D(y-y_j)$ are approximately related to the Dirac functions $\delta(x-x_i)$ and $\delta(y-y_j)$ in the following way:

$$D(x-x_i) \cong h_{i,j}\delta(x-x_i)$$

$$D(y-y_j) \cong h_{i,j}\delta(y-y_j). \tag{A4}$$